

Effect of Si barrier layers on the thermal stability of Al(1 wt.%Si)/Zr multilayers designed as EUV mirrors

Li Jia, Zhu Jie, Zhang Zhong, Qi Runze, Zhong Qi, Wang Zhanshan

(MOE Key Laboratory of Advanced Micro-Structured Materials, Institute of Precision Optical Engineering, School of Physics Science and Engineering, Tongji University, Shanghai 200092, China)

Abstract: To improve the thermal stability of Al/Zr multilayers, eighteen Al (1 wt.%Si)/Zr multilayers with different thickness (0.4 nm, 0.6 nm and 0.8 nm) of Si barrier layers were prepared by using the direct-current magnetron sputtering system. All the multilayers were annealed from 100 °C to 500 °C in a vacuum furnace for 1 h. To evaluate the effect of Si barrier layers on the thermal stability of Al/Zr system, the multilayers were characterized by grazing incidence X-ray reflectance (GIXR) and X-ray diffraction (XRD). From the alloy-interlayer model in the GIXR, the roughness of Al layer decreases with increasing thickness of Si barrier layers, while the roughness of Zr layer increases. Based on the XRD, the changing trends of crystal sizes of Al and Zr can explain the results in the GIXR. Comparing with the multilayers without Si barrier layers in the annealing process, the sample with Si barrier layer (0.6 nm) have better structural performance, of which the multilayers could have a stable structural performance above 300 °C.

Key words: Al/Zr multilayers; thermal stability; Si barrier layer; alloy-interlayer model

CLC number: O434.1 **Document code:** A **Article ID:** 1007-2276(2015)04-1335-08

Si 间隔层对 Al(1 wt.%Si)/Zr 极紫外多层膜热稳定的作用研究

李 嘉, 朱 杰, 张 众, 齐润泽, 钟 奇, 王占山

(同济大学 物理科学与工程学院 精密光学工程技术研究所
先进微结构材料教育部重点实验室, 上海 200092)

摘 要: 为了提升 Al/Zr 多层膜的热稳定性, 采用直流磁控溅射方法制备了 18 个带有不同厚度 Si 间隔层的 Al(1 wt.%Si)/Zr 多层膜, 并将这些样品分别进行了不同温度(100~500 °C)的真空退火, 退火时间为 1 h。利用 X 射线掠入射反射(GIXR)和 X 射线衍射(XRD)的方法来研究 Si 间隔层对 Al/Zr 多层膜热稳定性的作用。GIXR 测量结果表明: 随着 Si 间隔层厚度的增大, Al 膜层的粗糙度减小, 而 Zr 膜层的粗糙度增大; XRD 测量结果表明: Al 和 Zr 膜层粗糙度的变化是由于退火后膜层中晶粒尺寸不同造成的。相比于没有 Si 间隔层的 Al/Zr 多层膜, 引入厚度为 0.6 nm 的 Si 间隔层可以有效提升 Al/Zr 多层膜的热稳定性。

关键词: Al/Zr 多层膜; 热稳定性; Si 间隔层; 合金界面层模型

收稿日期: 2014-08-11; 修订日期: 2014-09-15

基金项目: 国家自然科学基金委员会与中国工程物理研究院联合基金资助(U1430131); 上海市科委纳米项目(11nm0507200)

作者简介: 李嘉(1988-), 女, 硕士生, 主要从事 X 射线多层膜光学方面的研究。Email: freya.lijia@foxmail.com

导师简介: 王占山(1963-), 男, 教授, 博士, 主要从事极紫外、软 X 射线及 X 射线光学方面的研究。Email: wangzs@tongji.edu.cn

0 Introduction

Al-based multilayers with high reflectivity have attracted much attention with the applications in extreme ultra violet (EUV) solar astrophysical imaging^[1-5]. Particularly, Al/Zr multilayers deposited on Si substrates are extremely of significance for the proposal of coating such multilayers on normal-incidence telescopes tuned to specific emission lines (i.e. Fe-IX($\lambda=17.1$ nm), Fe-XI($\lambda=18.0$ nm) and Fe-XII($\lambda=19.3$ nm)). In recent years, we have demonstrated that the Al (1 wt.% Si)/Zr multilayers have both good optical and structural performance, and thermal stability^[6-10]. Based on the experimental results, the interfacial roughness is small at the first 40 periods, and then increases while the period number is greater than 40. For the optical performance of Al(1 wt.% Si)/Zr with 40 periods, the experimental peak reflectivity is 41.2 % at 5° incidence angle, which is much lower than the corresponding theoretical value of 70.9% . The X-ray diffraction(XRD) and X-ray photoelectron spectroscopy (XPS) have revealed that the large differences between theoretical and experimental analysis are due to the four impact factors^[6-7], including inhomogeneous crystallization of aluminum, contamination of the multilayer, surface oxidized layer and interdiffusion between Al and Zr layers. In order to decrease the effect of inhomogenous crystallization of Al on the optical and structural properties of Al (1 wt.% Si)/Zr multilayers, Al was separated into several layers, and doped Si into Al layer to disfavor the crystallization of Al^[6]. The experimental reflectivity can be improved from 48.1% to 50% . Besides the inhomogeneous crystallization, serious diffusion happens during the annealed process which induces the decrease of EUV reflectivity and deterioration of thermal stability^[8]. There are two different diffusion processes: (1) the interdiffusion between the layers which changes the optical constant of Al/Zr multilayers; (2) the diffusion and newly formed

compounds makes the interface undistinguishable, and finally changes the structure^[9]. Taking into account the interaction between Al and Zr, interdiffusion and newly formed compounds from Al and Zr, we would like to hamper the interdiffusion between Al and Zr by inserting the barrier layer in Al (1 wt.% Si)/Zr multilayers, so that the thermal stability could be improved.

As a matter of fact, different types of barrier layers are investigated and widely applied to decrease interdiffusion^[11], smoothen the interface, increase the reflectivity^[12], and even improve the thermal stability^[13] in other multilayers. The materials of the diffusion barrier layer include Si, B₄C, and SiC et al. The barrier layers of B₄C and SiC are suitable for Mo/Si multilayers, however, they have different shortcomings for Al/Zr multilayer. For instance, the interface between B₄C and Al is indistinct, the stress of B₄C is larger, and the optical constant of B₄C affects the standing wave in Al/Zr multilayers. As compared to B₄C, the interface between Al and SiC is clearer, there are no new formed compounds in the interfaces, but the interdiffusion between SiC and Al could lower the reflectivity^[13]. As compared to different barrier layers mentioned above, Si has two advantages: (1) Si has the similar optical constant as Al; (2) the inserted Si barrier layer will disturb the crystallization of Al, which could decrease the roughness of Al layer and smooth the interface of Al/Zr^[8]. Considering these, Si could be a better option as barrier layers for Al/Zr multilayers in the wavelength range of $\lambda\sim 17-19$ nm.

In this paper, we shall investigate the effect of Si barrier layers on the thermal stability of the Al(1 wt.% Si)/Zr multilayers. The structural performances of the room temperature (RT) samples and annealed samples were characterized by grazing incidence X-ray reflectance(GIXR) and X-ray diffraction (XRD). The fitting data of two different four-layer models, (pure Si fitting model and alloy-interlayer model in the GIXR) are compared to show that the roughness of Al decreases with increasing thickness of Si barrier

layers, while the roughness of Zr increases. Moreover, the XRD measurements provide crystal orientations, grain sizes and peak positions for different annealed temperatures from 100 °C to 500 °C. From these analysis, the changes of roughness from the GIXR measurements are explained. Finally, the structural performances are also compared for the Al(1 wt.% Si)/Zr multilayers with/without Si barrier layers, it is shown that the inserted Si barrier can improve the thermal stability.

1 Experimental method

Eighteen Al(1 wt.% Si)/Zr multilayer samples are prepared by direct-current magnetron sputtering system^[6-7,14-15]. Each multilayer consisted of 40 bi-layers, with the periodic thickness around 9.7 nm. Before deposition, the base pressure was 8.0×10^{-5} Pa, and the samples were deposited on Si wafers under a 0.18 Pa argon(99.999 9% purity) pressure. The sputtering targets with diameter of 100 mm were zirconium(99.5%) and silicon doping in aluminum (Al(1 wt.% Si)).

The thermal stability of Al(1 wt.% Si)/Zr multilayers

with various Si barrier layers were evaluated, as shown in Tab.1, where the samples were annealed at the temperatures of 100 °C, 200 °C, 300 °C, 400 °C and 500 °C in a vacuum furnace for 1 h, respectively, as compared to those for RT. After annealing at different temperatures, the samples were cooled to room temperature naturally in a vacuum furnace with a base pressure of 3×10^{-4} Pa. In order to test the effect of Si barrier layer on the Al (1 wt.% Si)/Zr multilayers before and after annealing, we chose different thickness Si barrier layers of 0.4 nm, 0.6 nm and 0.8 nm, as shown in Tab.1. Since the thickness has equal difference in the region of 0–1 nm. The GIXR measurements was carried out by using an X-ray diffractometer working at the Cu K α line (0.154 nm). The fitting calculation of GIXR curves performed with Bede Refs software (genetic algorithm) is used to determine the individual layer thickness and interface roughness^[16]. In addition, XRD measurements further provides the identification of crystalline phases presented in the modified layer along with structural changes during the annealing temperatures.

Tab.1 Periodic length of the Al(1 wt.% Si)/Zr multilayer with Si barrier layers are derived from the GIXR measurements

Sample	Barrier/mm		Annealing temperature/°C					
			RT	100	200	300	400	500
Periodic length, D/nm	Si=0.4	Before annealing	10.1	10.0	10.0	10.0	10.1	10.1
		After annealing	10.1	10.0	10.0	9.9	9.9	9.8
	Si=0.6	Before annealing	9.5	9.5	9.5	9.4	9.4	9.4
		After annealing	9.5	9.5	9.5	9.4	9.3	9.3
	Si=0.8	Before annealing	9.7	9.6	9.5	9.4	9.4	9.4
		After annealing	9.7	9.6	9.5	9.3	9.3	9.2

2 Results

To estimate the initial structure of Al(1 wt.% Si)/Zr multilayer, the four-layer model (with pure Si interlayer or alloy interlayer) was used to fit the results of GIXR measurements. The estimated

thicknesses and roughness of the Al, Zr layers and interlayer with Si are listed in Tab.2. In the four-layer model, the composition of the interlayer is assumed to be pure Si. Figure 1 (a) shows that the fitting data with Si interlayer model does match well with the GIXR experimental results at the Bragg peaks, while

the matching quality is not good in the region between the Bragg peaks. Generally, this mismatch between the fitting data and experimental data may be due to the interdiffusion among Al, Zr and Si layers. The interaction between the Si barrier layer and Al or Zr layers may also formed the new compounds at the interfaces during the annealing process. Hence, three kinds of alloy-interlayer models, was used to fit the experimental results, in which the Al-on-Zr and Zr-on-Al interfaces are different: (1) two interlayers are both Al-Si alloying; (2) two interlayers are both Al-Zr-Si alloying. (3) Al-on-Zr interface and Zr-on-Al interface are used Al-Si alloying and Al-Zr-Si alloying, respectively. Among these models, the third fitting model is the most suitable for the GIXR experimental results, as shown in Fig.1 (b), since the growth of Si on the Al and Zr layers are quite different, and the information in the interfaces may be different^[6].

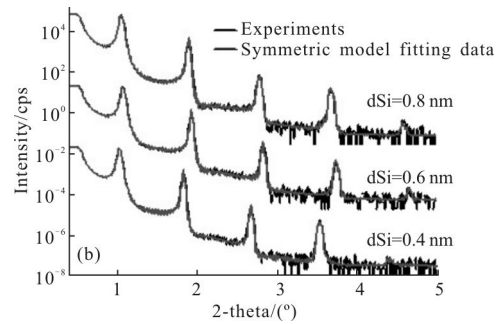
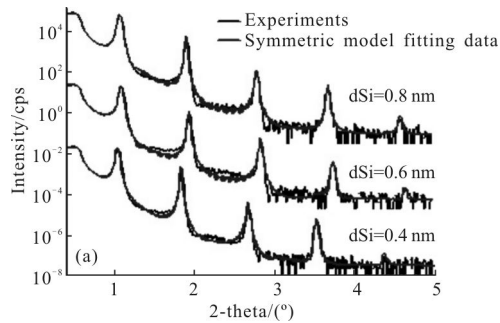


Fig.1 A comparison between the fitting results by using the pure Si interlayer model (a) and the alloy-interlayer model (b) for the samples of RT

As demonstrated in Tab.2, the roughness of different layers in pure Si interlayer model is larger than that in alloy-interlayer model. In alloy-interlayer model, the roughness of Al decreases with the thickness of Si barrier layer increasing. The roughness of Al is 0.84 nm, 0.80 nm, and 0.77 nm corresponding to different thickness of Si barrier layer, which is 0.4 nm, 0.6 nm and 0.8 nm. Whereas, the roughness of Zr increases with the thickness of Si barrier layer. The roughness of Zr is 0.75 nm, 0.81 nm, and 0.91 nm for corresponding thickness of Si barrier layer. Additionally, for the same thickness of Si barrier layer, the relative difference between roughness of the interlayers Al-on-Zr and Zr-on-Al in the pure Si interlayer model is always larger than that in alloy-interlayer model. From the comparison between two

Tab.2 Parameters deduced from the fit of sample curves using different models derived from Fig.1

Sample	(a) Si interlayer model			(b) Alloy-interlayer model		
	Layers	Thickness/nm	Roughness/nm	Layers	Thickness/nm	Roughness/nm
dSi=0.4 nm	Si	0.4	0.25	Al ₁ Zr _y Si _{1-x-y}	0.4	0.14
	Al(1 wt.% Si)	5.9	1.34	Al(1 wt.% Si)	5.9	0.84
	Zr	3.4	0.82	Al _x Si _{1-x}	0.4	0.15
	Si	0.6	0.30	Zr	3.4	0.75
dSi=0.6 nm	Al(1 wt.% Si)	5.2	1.16	Al ₁ Zr _y Si _{1-x-y}	0.6	0.20
	Si	0.6	0.33	Al(1 wt.% Si)	5.2	0.80
	Zr	3.1	0.99	Al _x Si _{1-x}	0.6	0.21
	Si	0.8	0.59	Zr	3.1	0.81
dSi=0.8 nm	Al(1 wt.% Si)	5.1	1.01	Al ₁ Zr _y Si _{1-x-y}	0.8	0.28
	Si	0.8	0.63	Al(1 wt.% Si)	5.1	0.77
	Zr	3.0	1.29	Al _x Si _{1-x}	0.8	0.30
				Zr	3.0	0.91

models, the alloy-interlayer model has better results than the pure Si fitting model, which implies that Al–Si–Zr alloying is formed during annealing process. Therefore, we assume that the reason on new formed compounds is relevant to the changes of Al and Zr crystallization.

As mentioned above, the alloy-interlayer model is applied to obtain the thickness and roughness by fitting the XRD measurement data for each annealed samples. The samples' roughness at RT and anneal temperatures 300 °C (or 400 °C) were compared. It is shown that for the 0.4 nm thickness barrier layers of Si, the roughness at anneal temperature 100–200 °C is similar to that at RT (i.e. the change is tiny), but

when the annealed temperature goes up to 300 °C, the changes of roughness become dramatical. For instance, for 0.4 nm thickness of barrier layer Al_xSi_{1-x} , the roughness increases from 0.15 nm to 0.23 nm. Similarly, for 0.6 nm and 0.8 nm thickness layers, the roughness go up to 0.38 nm and 0.54 nm, respectively. When the annealed temperature is 400 °C, which is twice of roughness at RT. In Tab.3, the thickness and roughness of one period at RT and critical temperatures are list, namely 300 °C (or 400 °C). The results imply that the inserted barrier layer has the regular effects on the anneal process, and thickness of barrier layer affects the thermal stability. We carry out XRD measurement as follows.

Tab.3 Layer thickness and roughness obtained from alloy-interlayer model for different samples (0.4 nm, 0.6 nm, 0.8 nm), where the values at RT and critical point (300 °C or 400 °C)

Layers	Annealed temperature	dSi=0.4 nm		Annealed temperature	dSi=0.6 nm		Annealed temperature	dSi=0.8 nm	
		Thickness /nm	Roughness /nm		Thickness /nm	Roughness /nm		Thickness /nm	Roughness /nm
$Al_xZr_ySi_{1-x-y}$		0.4	0.14		0.6	0.20		0.8	0.28
Al(1 wt.% Si)	RT	5.9	0.84	RT	5.2	0.80	RT	5.1	0.77
Al_xSi_{1-x}		0.4	0.15		0.6	0.21		0.8	0.30
WeZr		3.4	0.75		3.1	0.81		3.0	0.91
$Al_xZr_ySi_{1-x-y}$		0.4	0.21		0.6	0.38		0.8	0.41
Al(1 wt.% Si)	300 °C	5.7	3.2	400 °C	5.1	4.0	400 °C	4.9	3.8
Al_xSi_{1-x}		0.4	0.23		0.6	0.38		0.8	0.54
Zr		3.4	1.9		3.0	2.3		2.8	2.5

Figure 2 illustrates the diffraction curves of samples with different annealed temperatures (RT, 100 °C, 200 °C, 300 °C, 400 °C and 500 °C) to illustrate the crystallization in the annealed Al (1 wt.% Si)/Zr multilayers, where the thickness of barrier layer Si is 0.6 nm. In Fig.2, we observe that the Al<111> peaks do not change when the annealed temperatures increases from RT to 300 °C. But shift dramatically during the annealed temperature from 300 °C to 400 °C. Actually, the diffraction curves for Si barrier layers with other thicknesses (0.4 nm and 0.8 nm) can also be obtained, and the whole peak positions (2–theta) of all samples

are presented in Tab.4. For the thinner Si layer barrier, i.e. Si=0.4 nm, the changing point of Al<111> peaks is in the region of anneal temperature from 2000 °C to 3000 °C, and the position of peak shifts from 38.74° to 38.48°, which is similar to the case without Si layer barrier. And the Al<111> peaks start to shift during the annealed temperature changing from 300 °C to 400 °C while the thickness of Si layer barrier is also increased. When Si is 0.6 nm, the position of Al<111> peak shifts from 38.77° to 38.51° in the same region from 300 °C to 400 °C. This result is in agreement with Fig.2. Additionally, when the

thickness of barrier is increased up to 0.8 nm, the peak position for Al<111> changes from 38.72° to 38.48° in the region of anneal temperature from 300 °C to 400 °C. Therefore, the different regions of annealed temperature demonstrate that the suitable Si barrier layer can improve the thermal stability.

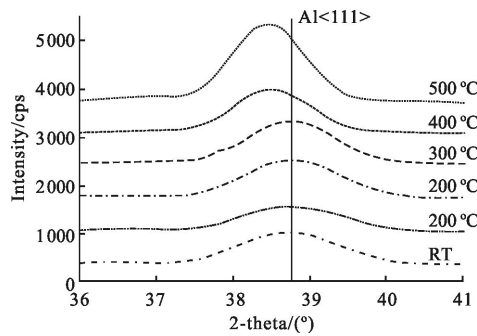


Fig.2 Diffraction curves of Al(1 wt.% Si)/Zr multilayers for different annealed from RT to 500 °C, with barrier layers of Si 0.6 nm thick

Tab.4 Crystal orientations, 2–theta of different annealing temperature samples

Sample	2–theta / (°)	Annealing temperature/°C					
		RT	100	200	300	400	500
dSi=0.4 nm	Al<111>	38.70	38.74	38.74	38.48	38.40	38.41
	Zr<101>	36.59	36.65	36.68	36.55	36.99	36.95
dSi=0.6 nm	Zr<002>	35.11	35.14	35.27	35.09	35.67	35.89
	Al<111>	38.75	38.80	38.80	38.77	38.51	38.49
dSi=0.8 nm	Zr<101>	36.54	36.50	36.50	36.89	36.89	36.85
	Zr<002>	-	-	-	-	-	-
dSi=0.8 nm	Al<111>	38.72	38.77	38.77	38.72	38.48	38.47
	Zr<101>	-	-	-	-	-	-
dSi=0.8 nm	Zr<002>	-	-	-	-	-	-

Based on the Scherrer formula [7], the crystal orientations and grain sizes of the samples are presented in Tab.5. The crystal size of Al <111 > decreases with Si barrier layer thickness increasing for different annealing temperatures. Since Si barrier layer interacts with and diffuses into Al layer, it finally disfavors the crystallization of Al. The large crystal size results in the interfacial roughness could also increase [1,7], which is consistent with the fitting data in alloy-interlayer model seen in Tab.1. On the contrary,

for the Zr plane, the crystal size of Zr<101> just increase with the thickness of Si barrier layer, and then decrease when thickness of Si barrier is rising up to 0.8 nm. But that of Zr<002> is only detected for 0.4 nm, because the intensity of X–ray is not strong enough. It seems that a suitable thickness of Si barrier layer can enhance the crystallization of Zr, but the thicker Si barrier layer may make more Si penetrate into Zr layer and finally decrease the crystallization of Zr. Thus, the XRD measurement provides the explanation of the roughness changes observed from GIXR measurement using the alloy-interlayer model. Besides, from XRD measurement and alloy-interlayer model that there exist new formed compounds, and the thickness and roughness change correspondingly. Actually, XRD measurements tell us that for the thickness of Si barrier layer, 0.4 nm, the peak of X–ray diffraction curves for Al(1 wt.% Si)/Zr multilayers shifts when the annealed temperature is between 200 °C and 300 °C. However, for other thickness, 0.6 nm and 0.8 nm, the peak of diffraction curves shifts for the annealed temperature from 300 °C to 400 °C. Therefore, we compare the results of the samples with and without Si barrier layers to see how Si barrier layer affects the thermal stability,

Tab.5 Crystal orientations, grain sizes of different annealing temperature samples

Sample	Crystal Grain/nm	Annealing temperature/°C					
		RT	100	200	300	400	500
dSi=0.4 nm	Al<111>	5.8	5.8	5.9	6.3	7.6	8.8
	Zr<101>	12.0	12.2	12.3	12.3	12.5	14.1
	Zr<002>	4.9	5.3	10.3	11.3	11.7	13.4
dSi=0.6 nm	Al<111>	4.4	4.6	4.7	4.9	6.8	7.8
	Zr<101>	12.6	12.8	13.1	13.3	13.6	14.2
	Zr<002>	-	-	-	-	-	-
dSi=0.8 nm	Al<111>	4.1	4.3	4.5	4.7	6.6	7.7
	Zr<101>	-	-	-	-	-	-
	Zr<002>	-	-	-	-	-	-

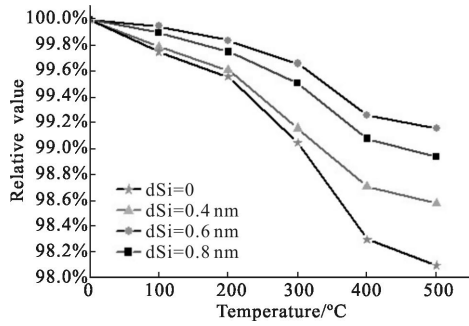


Fig.3 Relative periodic length of Al(1 wt.% Si)/Zr multilayer samples as a function of annealing temperature for different Si barrier layers(The periodic lengths were normalized by those of the samples before annealing in Tab.1)

3 Discussion

The experimental results described above illustrate that the results for Al (1 wt.% Si)/Zr multilayers with thin Si barrier layer are almost the same as those for the sample without Si barrier layer, while the behaviors of the samples with thickness of Si barrier layer, 0.6 nm and 0.8 nm are quite similar. In order to find the best thickness of Si barrier layer, the relative periodic length and diffraction peaks of Al(1 wt.% Si)/Zr multilayer samples with different thickness of barrier layer are compared. The relative periodic length of samples are displayed as a function of annealing temperature, as shown in Fig.3, where the periodic lengths were normalized by those of the samples at RT in Tab.1. For the Al (1 wt.% Si)/Zr multilayer without Si barrier layer, the relative value changes from 99.56% to 99.05% during the annealed temperature from 200 °C to 300 °C, and it is dramatically decreased to the 98.10% at the annealed temperature 500 °C. Experimental results from Fig.3 demonstrate that for the Al (1 wt.% Si)/Zr multilayer samples without Si barrier layer and with Si barrier of 0.4 nm thick, the critical point of changes for periodic thickness happens at the annealed temperature from 200 °C to 300 °C, while for the thickness of Si barrier layer, 0.6 nm and 0.8 nm, the critical point shifts to the region from 300 °C to 400 °C. In this case, when

the annealed temperature is up to 500 °C, the relative change of period thickness is 1.90% for the sample without Si barrier layer, and for other thickness Si barrier layer (0.4 nm, 0.6 nm and 0.8 nm), the relative changes are 1.42%, 0.84%, and 1.06%, respectively. Comparison demonstrates that the corresponding relative changes of 0.6 nm Si barrier layer are smallest.

To illustrate the thermal stability of the samples with inserted Si barrier layer, we further compare the XRD data. As shown in Fig.4, the positions of diffraction curves are as a function of annealing temperatures for various thicknesses Si layer. When the thickness of Si layer barrier is 0.4 nm, the diffraction peaks change during the annealing temperatures up from 200 °C to 300 °C, which are the similar to the behavior for Al(1 wt.% Si)/Zr multilayer without Si barrier layer. However, for other thickness of 0.6 nm and 0.8 nm, the critical point shifts to the region of the annealing temperatures from 300 °C to 400 °C. Due to the compounds changing in the alloy interlayers during the annealed process, resulting peaks of X-ray diffraction curves are shift^[6]. Combing the structural performance discussed above, the sample with Si barrier layer (0.6 nm) has better structure performance, and the multilayers could have a stable structure performance above 300 °C.

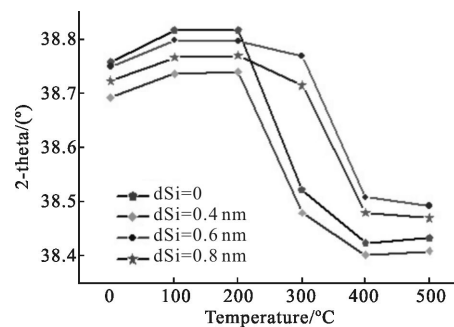


Fig.4 Diffraction peaks versus annealing temperatures for various thicknesses of Si barrier layer(Si=0, 0.4, 0.6, and 0.8 nm)

4 Conclusion

To evaluate the effect of Si barrier layers on the thermal stability of Al multilayer, we prepare eighteen

Al (1 wt.% Si)/Zr multilayers with different thickness barrier layers of Si 0.4, 0.6 and 0.8 nm. The multilayers are annealed from 100 °C to 500 °C in a vacuum furnace for 1h. The pure Si layer model and alloy-interlayer model are applied to fit the data from GIXR measurement. From the comparison between two fitting models, we notice that the alloy-interlayer model is better. For the 0.4 nm thickness of Si layer, the change of roughness becomes dramatic when the annealed temperature is higher than 300 °C, while for other thickness (0.6 nm and 0.8 nm), the roughness changes dramatically above 400 °C. The XRD measurement is further carried out, it is found that Si barrier layer can hamper the crystallization of Al, and the reasonable thickness barrier layer of Si can improve the crystallization of Zr. The thicker Si barrier layer (i.e. 0.8 nm) penetrates into Zr layer, and disfavors the crystallization of Zr eventually. Moreover, the relative periodic length and X-ray diffraction peaks of Al (1 wt.% Si)/Zr multilayer samples with different thickness of barrier layer are compared. As a result, the Si barrier layer can improve the thermal stability and the thickness of 0.6 nm is the best option for Al (1 wt.% Si)/Zr multilayers designed as EUV mirrors.

References:

- [1] Windt D L, Bellotti J A. Performance, structure, and stability of SiC/Al multilayer films for extreme ultraviolet applications [J]. *Appl Opt*, 2009, 48(26): 4932–4941.
- [2] Jonnard P, Le Guen K, Hu M -H, et al. Optical chemical, and depth characterization of Al/SiC periodic multilayers [C]//SPIE, 2009, 7360: 73600O.
- [3] Meltchakov E, Hecquet C, Roulliy M, et al. Development of Al-based multilayer optics for EUV [J]. *Appl Phys A*, 2010, 98(1): 111.
- [4] Hu M H, Guen K L, André J -M, et al. Structural properties of Al/Mo/SiC multilayers with high reflectivity for extreme ultraviolet light [J]. *Opt Express*, 2010, 18 (19): 20019–20028.
- [5] Meltchakov E, Ziani A, Auchere F, et al. EUV reflectivity and stability of tri-component Al-based multilayers [C]//SPIE, 2011, 8168: 816819.
- [6] Zhong Q, Li W B, Zhang Z, et al. Optical and structural performance of the Al/Zr reflection multilayers in the 17–19 nm region[J]. *Opt Express*, 2012, 20(10): 10692–10700.
- [7] Zhong Q, Zhang Z, Zhu J T, et al. The chemical characterization and reflectivity of the Al (1.0% wtSi)/Zr periodic multilayer [J]. *Appl Surf Science*, 2012, 259: 371–375.
- [8] Zhong Q, Zhang Z, Zhu J T, et al, The thermal stability of Al (1%wtSi)/Zr EUV mirrors [J]. *Appl Phys A*, 2012, 109 (1): 133–138.
- [9] Voronov D L, Anderson E H, Cambie R, et al. A 10,000 groove/mm multilayer coated grating for EUV spectroscopy [J]. *Opt Express*, 2011, 19(7): 6320–6325.
- [10] Voronov D L, Anderson E H, Cambie R, et al. Roughening and smoothing behavior of Al/Zr multilayers grown on flat and saw-tooth substrates[C]//SPIE, 2011, 8139: 81390B 1–10.
- [11] Pershyn Y P, Zubarev E N, Kondratenko V V, et al. Reactive diffusion in Sc/Si multilayer X-ray mirrors with CrB₂ barrier layers[J]. *Appl Phys A*, 2011, 103(4): 1021–1031.
- [12] Hu Minhui, Guen K L, André J -M, et al. Structural properties of Al/Mo/SiC multilayers with high reflectivity for extreme ultraviolet light [J]. *Opt Express*, 2010, 18 (19): 20019–28.
- [13] Jonnard P, Maury H, Guen K L, et al. Effect of B₄C diffusion barriers on the thermal stability of Sc/Si periodic multilayers[J]. *Surf Science*, 2010, 604(S11–12): 1015–1021.
- [14] Wang F L, Wang Z S, Zhang Z, et al. W/B₄C, W/C, W/Si multilayers [J]. *Opt Precision Eng*, 2005, 13: 28–33. (in Chinese)
- [15] Wormington M, Panaccione C, Matney K M, et al. Characterization of low-Z material layer profiles in bilayer structures by X-ray reflectivity measurement [J]. *Opt Precision Eng*, 2007, 15: 1838–1843.
- [16] Matthew W, Charles P, Kevin M, et al. Characterization of structures from X-ray scattering data using genetic algorithms [J]. *Philos Trans R Soc Lond*, 1999, A357: 2827–2848.